Magnetic Ordering of DNA Liquid Crystals[†]

Rolf Brandes and David R. Kearns*

Department of Chemistry, University of California at San Diego, La Jolla, California 92093

Received March 3, 1986; Revised Manuscript Received May 15, 1986

ABSTRACT: Sonicated calf thymus DNA with an average length of ~100 base pairs has been found to form a cholesteric liquid crystal at a concentration of ~250 mg of DNA/mL of solution. Immediately after preparation, small ordered domains of a few micrometers are formed, resulting in an opaque solution. This liquid crystal can readily be oriented in the magnetic field of an NMR magnet, resulting in a clear birefringent phase. The DNA molecules align with their helix axes perpendicular to the field so that the cholesteric pitch axis was parallel with the field. A pitch length of ~2.5 μm for the cholesteric phase was determined both from optical measurements (optical light rotation) and from NMR measurements (solvent diffusion). The observation that DNA molecules can be magnetically oriented opens up new possibilities for studying the structure and dynamics of the aligned DNA molecules.

It has been known for some time that DNA and RNA solutions can spontaneously undergo a transition to a liquid crystalline state above a critical concentration (Robinson, 1961; Iizuka, 1977, 1978a,b; Iizuka & Yang, 1978; Iizuka & Kondo, 1979; Senechal et al., 1980; Trohalaki et al., 1984). Although the critical concentrations are high (>50 mg/mL for short DNA), we note that the local concentration of DNA in vivo can also be quite large, and liquid crystal formation may possibly play some role in packaging DNA in certain systems. Studies of DNA liquid crystals are also of intrinsic interest in terms of the liquid crystal forming properties of polyelectrolytes (DuPre & Samulski, 1979).

The first report that high molecular weight DNA might form a liquid crystal was made by Robinson (1961), who suggested that the phase was of the cholesteric type. DNA and RNA liquid crystals were further studied by Iizuka (Iizuka, 1977, 1978a,b; Iizuka & Yang, 1978; Iizuka & Kondo, 1979), and shorter fragments of RNA were investigated by Senechal et al. (1980), who found a liquid crystal structure that was not of the simple cholesteric type. Concentrated solutions of DNA fragments [147 base pairs (bp), ~175 mg/mL] in the liquid crystalline phase have recently been studied by Rill et al. (1983). From NMR measurements, they concluded that certain motions of the DNA backbone were frozen out at the phase transition to the liquid crystal state. Lower concentrations of DNA (~15 mg/mL) also undergo a type of gel transition (Fried & Bloomfield, 1984), but a liquid crystal phase is only predicted for much higher concentrations according to the theory of Onsager (1949).

Since many liquid crystals become ordered by the application of a magnetic field, it was not surprising that Iizuka observed magnetic field effects on the optical properties of RNA liquid crystals (Iizuka, 1978a,b; Iizuka & Yang, 1978; Iizuka & Kondo, 1979). This suggests that DNA liquid crystals might also be oriented in a magnetic field, although an earlier NMR study of concentrated DNA solutions gave no evidence for such effects (Rill et al., 1983).

In this study, we have investigated the effects of magnetic fields on the structure and properties of DNA liquid crystals using both optical and NMR methods. In our experiments with short (~100 bp) DNA fragments we found a certain critical concentration (~170 mg/mL) where the solution became biphasic at room temperature. At higher concentrations (~240 mg/mL) a strongly birefringent one-phase system is observed, which has a transition to an isotropic phase without optical activity at elevated temperatures. This behavior is typical of lyotropic liquid crystals (DuPre & Samulski, 1979) and will be described elsewhere. With DNA contained in a microslide, optical properties such as microscopic texture, light rotation, and light diffraction were studied as a function of the direction of the induced alignment by the magnetic field. ^{2}H NMR was used to study the interaction of "bound" solvent molecules (D_2O) with the DNA superstructure over a range of temperatures, including temperatures where the bulk solvent was frozen. This method can be used to determine the order and type of phase simply from the general line shape. More detailed information is also obtained since the path length for diffusion of D_2O, on the time scale of the NMR measurement (inverse of the natural line width), was found to be of the same order of magnitude as the cholesteric pitch length.

The observation that magnetic fields can be used to align small DNA fragments may be particularly useful in obtaining macroscopically oriented DNA samples for studies of structural and dynamical properties of DNA itself (Vold et al., 1986).

EXPERIMENTAL PROCEDURES

High molecular weight calf thymus DNA (Sigma No. D-1501) was sonicated for 5 h with a Branson sonicator (Model W-375) to reduce the molecular weight (Granot et al., 1982). The average length was estimated from gel electrophoresis to be ~100 bp with a distribution of ±50 bp (80% of material). Repeated phenol extractions were employed to reduce any residual proteins. The total NaCl concentration in the final sample was controlled by equilibrating precipitated DNA in a 73% EtOH/H_2O bath containing 0.032 M NaCl to obtain an excess of 1.3 mg of NaCl/100 mg of dry DNA (Rupprecht & Forslind, 1970). Dissolving 28 mg of freeze-dried DNA per 100 μL of D_2O buffer (0.004 M cacodylic acid, 0.002 M ethylenediaminetetraacetic acid (EDTA), p*D* 7.0) gave a DNA solution with a concentration of 248 ± 10 mg of dry DNA/mL of solution containing 0.06 M NaCl. [This corresponds to a solute partial specific volume of 0.47 cm^3 g^{-1} for the DNA, in close agreement with earlier measurements

---

[†] This work was supported by a grant from the National Science Foundation (Grant DMB 83-03374 to D.R.K.) and by a travel grant to R.B. from the Department of Biophysics, University of Stockholm.

0006-2960/86/0425-5890$01.50/0

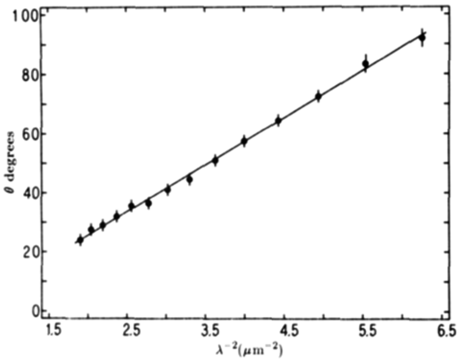

FIGURE 1: Rotation of light as a function of wavelength for a liquid crystal of DNA (C = 248 mg/mL) in a 400-μm-thick microslide.

of 0.53 $cm^3\ g^{-1}$ (Tanford, 1961).] The concentration was checked by measurement of UV absorbance (at 260 nm) and found to be 235 ± 10 mg of dry DNA/mL of solution.

Microphotographs of oriented DNA in a microslide ("precision rectangle glass capillary tubing", Vitro Dynamics Inc.) were obtained with a Zeiss photomicroscope (III) using crossed polarizers. This microscope was also used to obtain the pitch length of the cholesteric liquid crystal by measuring the distance between the periodic diffractive minima (Robinson, 1961). A Unitron (Model MPS-2) microscope illuminated with white light filtered through a Bauch & Lomb (Model 33-86-02) monochromator was used to determine the rotation of light. By rotating the bottom polarizer for maximum extinction, we determined the optical rotation as function of wavelength.

An independent measurement of the pitch length was also performed with a Hughes 5-MW helium–argon laser (λ = 638.2 nm) to obtain a diffraction pattern from an aligned DNA liquid crystal.

Spectra of D_2O were obtained on a homebuilt ^2H NMR spectrometer operating at 38.4 MHz with the 5-mm solenoid coil mounted with its axis perpendicular to the 5.9 T applied magnetic field. The reported spectra were obtained by a phase-cycled $\pi/2_x$–τ_1–$\pi/2_y$–τ_2–acq quadrupolar echo sequence (Davis et al., 1976) with a $\pi/2$ pulse of 2.8 μs and delay times $\tau_1 = \tau_2 = 100$ μs.

RESULTS

Optical Experiments. When a 248 mg/mL DNA solution was placed in a 400 μm path length microslide, a strong birefringence was observed when viewed through crossed polarizers. A polarizing microscope revealed small domains (tenths of a millimeter) with different colors. Use of a smaller path length (50 μm) gave a uniform area with "oily streaks" (Demas & Richter, 1978). If the sample is left to dehydrate for a couple of days, rodlike crystallites developed, the smallest having a diameter of 1–3 μm and a length of 20–40 μm. The sample in the 400-μm slide (sealed) also developed uniform areas that increased in size with time. The color of these areas depends on the angle between the crossed polarizers, and they show a wavelength-dependent rotation of light (Figure 1). When the slide was placed in a magnetic field with the cover glass perpendicular to the field of an NMR magnet (5.9 T), the entire slide became clear and developed a uniform light-rotating area within a few seconds, instead of several days. This new state was stable for weeks even when the sample was removed from the field. A microphotograph obtained on such a sample is shown in Figure 2 (top).

If the slide is placed in the magnetic field with the cover glass oriented parallel to the field, a different structure is formed. After the sample is removed from the field, a granular structure is observed in the microscope [Figure 2 (bottom)]. (If the sample is observed a day later, a multiple-banded structure sometimes developed with bands ~30 μm broad perpendicular to the field.) Perpendicular to the direction of the aligning magnetic field, equidistant, alternating, parallel dark and bright lines were also observed with or without the polarizers (not shown). The lines had a spacing S = 1.2 μm (distance between two dark bands) and only had a few dislocations where they were not perfectly perpendicular to the magnetic field. Similar periodic lines have been observed with high molecular weight DNA (Robinson, 1961), but the arrangement of lines was found to be random since no magnetic alignment was introduced. A striking feature of this structure is the linear polarizing power of the slide (as determined by viewing the slide through a linear polarizer) and the bright iridescent colors. The slide reflects a spectrum of colors when a beam of white light is incident at an angle to the surface. Alternatively, white light can be diffracted into its spectral components by shining the light at a right angle through the slide. To quantitatively determine the diffracting properties of the DNA liquid crystal, monochromatic light (λ = 638 nm) was used to create a diffraction pattern (first order). This resulted in a band of light perpendicular to the direction of the aligning magnetic field on each side of the central spot from the undiffracted light beam. The angle of diffraction for the first-order band was determined to θ = 36°. This diffraction is clearly an indication of the formation of an ordered system.

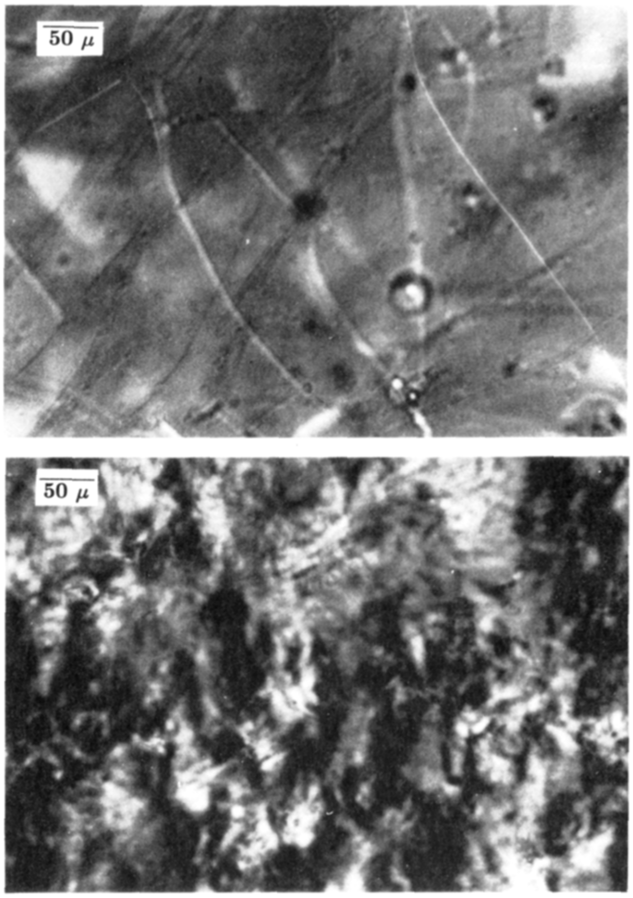

FIGURE 2: Microphotograph of DNA (C = 248 mg/mL) in a 400-μm-thick microslide. DNA oriented with cover glass (top) perpendicular to magnetic field (5.9 T) and (bottom) parallel to field.

NMR Experiments. When the concentrated DNA solution was placed in a 5-mm NMR tube (Wilmad 512-RP), the sample was opaque due to light scattering of an isotropic

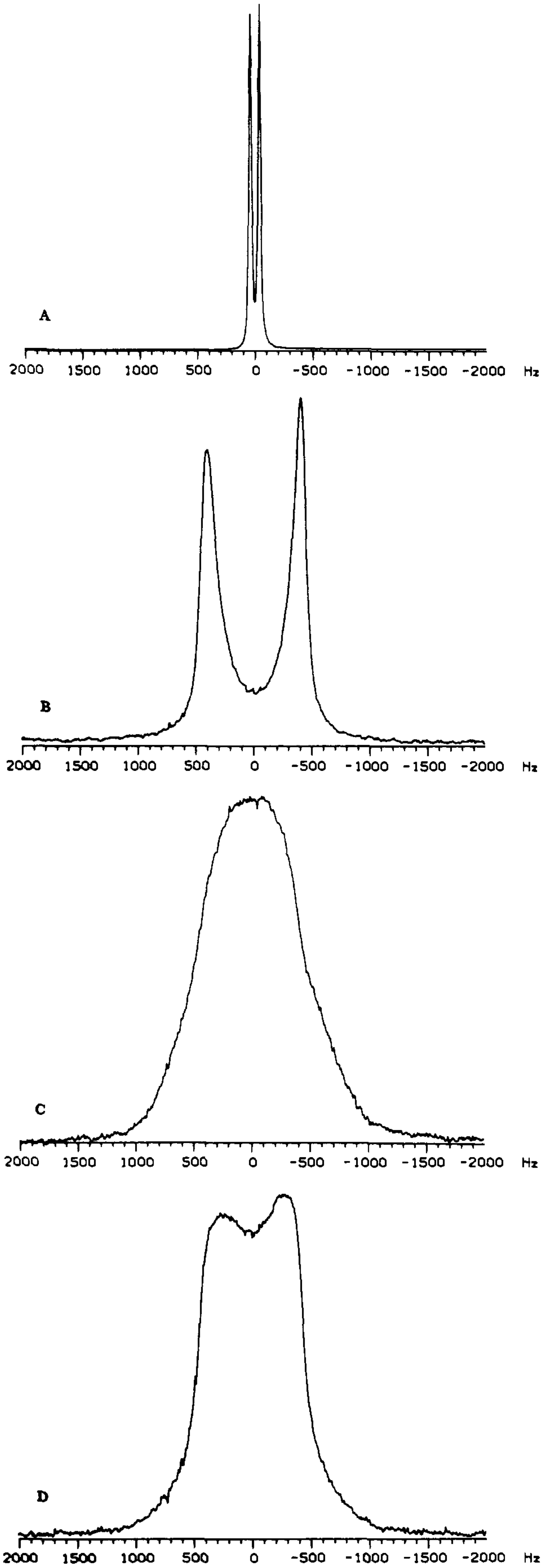

FIGURE 3: ^{2}H NMR spectra of D_2O in a DNA liquid crystal (C = 248 mg/mL): (A) unfrozen (T = 25 °C), aligned by field; (B) frozen (T = −11 °C) while aligned in the field; (C) frozen (T = −11 °C) while aligned in the field, and then rotated 90°; (D) frozen (T = −11 °C) outside field, resulting in an unaligned sample.

distribution of small ordered units. As with the microslide, the sample in the NMR tube shows a slow (couple of days) macroscopic ordering outside the field as it starts to form clear, birefringent regions (usually starting from the bottom of the tube). A completely clear solution is obtained within a few seconds if the axis of the sample tube is positioned perpendicular to the magnetic field (except near the walls on the side of the tube, parallel with the field lines). Once formed, this clear phase can be retained for at least several weeks outside the field if not shaken or heated. The ^{2}H spectrum in Figure 3A shows the residual anisotropy of the D_2O solvent in this ordered phase, resulting in a quadrupolar splitting of 115 Hz. To obtain the splitting of the ^{2}H resonance at other angles of orientation of the liquid crystal with respect to the field, the sample tube needs to be rotated. Unfortunately, the time scale for realignment of the DNA molecules with respect to the field is faster than the time needed for the NMR measurements (a few seconds). However, freezing the sample in the field traps the DNA, and realignment is then hindered as the sample is rotated.

As the temperature is lowered from 25 to −10 °C, the splitting in the ^{2}H spectrum remains constant, but between −10 and −11 °C, the sample freezes and the splitting abruptly increases from 115 to 815 Hz (Figure 3B). The integrated signal intensity from the unfrozen D_2O then contributes only ~23% of the intensity of the unfrozen sample (i.e., 0.8 g of D_2O/g of dry DNA or ~27 D_2O molecules/base pair is observed).

The spectrum obtained from an aligned frozen sample that has been rotated by 90° (shown in Figure 3C) resembles that of a partially averaged cylindrical powder pattern. A different type of powder spectrum was obtained (Figure 3D) when the sample was first heated outside the field to convert it to its isotropic phase and then frozen outside the field. This procedure is expected to produce a sample with isotropically distributed, ordered regions. From this, it is clear that the freezing procedure does not dislocate the aligned DNA molecles to any appreciable degree.

DISCUSSION

All the results from the optical and NMR measurements are consistent with the DNA liquid crystal being of the cholesteric type as originally suggested by Robinson (1961). We will, therefore, discuss some properties of this phase and compare it with similar results obtained on other cholesteric systems.

Optical Experiments. According to the simplified theory of de Vrie, the optical rotation θ of light per unit length of material for a cholesteric phase with the pitch axis parallel with the beam of light (wavelength λ) can be expressed as (Robinson, 1961)

$$\theta = -\frac{2\pi n^2 P}{8\lambda^2(1 - \lambda^2/P^2N^2)} \qquad (1)$$

where P is the pitch length of the structure, n is the birefringence of the untwisted material, and N is the average diffractive index. If $\lambda^2/P^2N^2 \ll 1$, then the measured rotation θ_m is given by

$$\theta_m = \frac{-n^2 P}{\lambda^2} t \times 45 \text{ deg} \qquad (2)$$

where t is the thickness of the sample. When $\lambda^2/P^2N^2 \sim 1$, eq 1 predicts that the optical rotation becomes infinite and changes sign as λ increases. That this is not the case for the range of λ used here is evident in Figure 1 (sample oriented with cover glass perpendicular to the field), which shows a linear relationship as predicted by eq 2. Since the pitch axis must be aligned perpendicular to the plane of the cover glass for light rotation to occur, the DNA molecules are orienting at right angles to the field. The pitch length is given by 2·S, where S is the distance between two planes of the same refractive index. From the sample oriented in the field with the cover glass parallel with the field (DNA molecules oriented in planes perpendicular to the cover glass), S was measured from the spacing between the periodic lines to be 1.2 μm, so $P = 2.4$ μm. An independent measure of S can be obtained from the diffraction experiment. The diffraction from a grating is given by (Fowles, 1975)

$$n\lambda = d \sin \theta_n \tag{3}$$

where n is the order of the diffraction, λ is the wavelength of light, θ_n is the angle of the nth-order diffracted beam, and d is the spacing between the slits in the grating. In our case, the periodic variations in the diffractive index perpendicular to the beam correspond to the slits (i.e., S = d). From the measured diffraction angle $\theta_1 = 36°$, the calculated period S = 1.1 μm is in accordance with the microscope measurements. Since $P \sim 2.4$ μm, $\lambda^2/P^2N^2 \sim 0.02 \ll 1$ ($\lambda = 0.5$ μm, $N^2 \sim 2$ (S. Lindsey, personal communication)) as was required for eq 2 to be valid.

The slope in Figure 1 is given by eq 2 as

$$\frac{\mathrm{d}\theta_\mathrm{m}}{\mathrm{d}\lambda^{-2}} = -n^2 Pt \times 45 \tag{4}$$

A slope of 15.8 ± 0.4 deg ·μm^2 is obtained from the graph, so $|n^2P| = (8.8 \pm 0.2) \times 10^{-4}$ μm. Therefore, the birefringence of the untwisted material (i.e., uniaxially oriented) is $n = 0.02 \pm 0.005$. The birefringence measured in oriented fibers of high molecular weight DNA is $n \sim 0.04$ (S. Lindsey, personal communication). This is in fair agreement with the more dilute (~2.5 times) liquid crystal measured here.

NMR Experiments. In an ordered uniaxial phase, the spectrum of a single deuterium nucleus of the D_2O solvent consists of a doublet whose total splitting is related to the order parameter S_OD of the OD-bond by (Halle & Wennerström, 1981)

$$\Delta\nu_Q = \frac{3}{4}\left(\frac{e^2qQ}{h}\right)|(3 \cos^2 \theta - 1)S_\mathrm{OD}| \tag{5a}$$

where

$$S_\mathrm{OD} = \frac{1}{2}(3 \cos^2 \alpha - 1 + \eta \sin^2 \alpha){S_0}^2 - \frac{1}{2(6)^{1/2}}[3 \sin^2 \alpha + \eta(\cos^2 \alpha + 1)]{S_2}^2 \tag{5b}$$

Here $e^2qQ/h = 213$ kHz is the deuterium quadrupole interaction constant (Waldenstein et al., 1964), θ is the angle between the magnetic field and the director, α is one-half of the DOD angle of water molecules, $\eta \sim 0.11$ is the asymmetry parameter (Waldenstein et al., 1964), and ${S_0}^2$ and ${S_2}^2$ are second-rank order parameters related to the Wigner rotation matrices (Halle & Wennerström, 1981). For a rapidly moving D_2O molecule ($\tau^{-1} \ll e^2qQ/h$) that probes all possible different sites in the uniaxial phase, averaging over α takes place so that

$$\Delta\nu_Q = \frac{3}{4}\left(\frac{e^2qQ}{h}\right)|(3 \cos^2 \theta - 1)\langle S_\mathrm{OD}\rangle| \tag{6}$$

where $\langle S_\mathrm{OD}\rangle$ is the averaged order parameter.

In the D_2O spectrum of the DNA liquid crystal at room temperature (Figure 3A) a two-line spectrum is obtained with a splitting of $\Delta\nu_Q = 115$ Hz. Since the optical measurements showed that the DNA molecules orient perpendicular to the magnetic field, $\theta = 90°$, and therefore $\langle S_\mathrm{OD}\rangle = 0.7 \times 10^{-3}$. When the sample freezes (Figure 3B), solvent molecules in the primary hydration shell remain unfrozen (Falk et al., 1970), and since these are better oriented than the bulk solvent the averaged order parameter $\langle S_\mathrm{OD}\rangle$ increases. A splitting of $\Delta\nu_Q = 810$ Hz corresponds to $\langle S_\mathrm{OD}\rangle = 0.5 \times 10^{-2}$. The trailing inside edge of the doublet is attributed to a Gaussian distribution ($\sigma = 10°$–$15°$) of DNA molecule orientations at $\theta = 90°$ (Luz et al., 1981).

Senechal et al. (1980) found that the Cotton–Mouton constant for the liquid crystal of poly(A)·poly(U) was smaller than expected for the case where all RNA helices were aligned perpendicular to the magnetic field. They suggested a possible model for the three-dimensional spatial arrangement of the rodlike helices with only 25% more RNA molecules oriented perpendicular to rather than parallel with the field. Their model for the RNA packing does not fit with our results on the DNA liquid crystal since only one doublet resonance (corresponding to $\theta = 90°$) is observed. However, from the NMR data we cannot exclude the possibility of a fraction of randomly oriented domains (<50%) (Luz et al., 1981), even though this seems unlikely in view of the optical measurements which showed a well-aligned sample with the periodic layer lines perpendicular to the magnetic field.

It is interesting to compare our liquid results with those obtained from fibers of B-DNA oriented perpendicular to the applied field. Extrapolating these latter measurements at 25 °C to the same level of hydration as the frozen liquid crystal, we obtain a value of $\Delta\nu_Q = 600$ Hz (R. Brandes, R. R. Vold, R. L. Vold, & D. R. Kearns, unpublished results). A reduction of the splitting at $T = 25$ °C is expected since the splitting decreases with increasing temperature (R. Brandes et al., unpublished results).

If the frozen liquid crystal is rotated 90°, the cholesteric nature of the phase becomes apparent as shown in Figure 3C. The cylindrical powder pattern arises from the D_2O that is ordered by the DNA molecles which in turn are packed into planes oriented parallel to the field. Since the DNA in each plane have a different director orientation with respect to the field, a cylindrical powder pattern is expected. The observed spectrum is partially averaged due to diffusion of the D_2O solvent between the planes (along the pitch axis) (Luz et al., 1981; Chidichimo et al., 1982). Since the spectrum in Figure 3B could be best fitted with a (Gaussian) distribution of orientations, this will also affect the cylindrical pattern. A reduced intensity of the outer doublet corresponding to DNA helices that are parallel with the field is to be expected.

Certain cholesterogenic liquid crystals have been shown to form a special type of phase called the blue phase just below the transition temperature to an isotropic phase (Helfrich, 1979). Even though the "blue phase" exhibits high optical activity, it is optically isotropic and does not show birefringence. The spectrum in Figure 3D was obtained from an isotropic distribution of domains and is identical with the blue phase type spectrum (Collings & McColl, 1978; Samulski & Luz, 1980). Similar spectra have also been observed for DNA samples that have been slowly dried and then rehydrated (R. Brandes et al., unpublished results). That it is not a true blue phase is evident from the strong birefrigence of the unfrozen sample.

In general, an isotropic distribution of cholesteric domains will give rise to a powder pattern if the rotational diffusion constant D_R of the D_2O molecules along the pitch axis is small enough ($D_R \ll 2\pi\Delta\nu_Q$) (Luz et al., 1981). For higher diffusion rates, the splitting of the outer doublet is reduced, and the inner doublet, the "horns", broadens ($D_R \sim 0.2\pi\Delta\nu_Q$). If the diffusion rate is large enough ($D_R \gg 2\pi\Delta\nu_Q$), a collapsed powder pattern results with half the original width. It should be noted that the doublet from the horns always is visible in the spectrum. The outer doublet is only absent in a narrow range of diffusion rates ($0.2\pi\Delta\nu_Q < D_R < 2\pi\Delta\nu_Q$) when they coincide with the horns.

When the isotropically prepared DNA sample with the spectrum shown in Figure 3D was slowly heated, the spectrum started to collapse, resulting in an isotropic line at 0 °C (line width ~ 220 Hz). To account for this, the domain size of the cholesteric units must be small enough to allow for lateral diffusion between differently oriented domains.

Spectral simulations of the effects of diffusion in cholesteric liquid crystals have been performed by Luz et al. for both cylindrical powder patterns (Luz et al., 1981) and for blue phase type spectra (Samulski & Luz, 1980). For translational diffusion

$$2D_T\tau = \overline{x^2} \qquad (7)$$

and for rotational diffusion

$$2D_R\tau = 1 \qquad (8)$$

where D_T is the translational diffusion constant, x is the effective diffusion distance, and τ is the correlation time for respective diffusion type. For a molecule that diffuses along the pitch axis, the translational and rotational diffusion can be related since

$$x = P/\pi \qquad (9)$$

where P is the pitch length. Combining eq 7–9 gives

$$P = \pi(D_T/D_R)^{1/2} \qquad (10)$$

For a molecule that also diffuses (isotropically) to other isotropically ordered domains, P corresponds to an "effective" diffusion length. From the simulations cited above, the best fit to our spectra is obtained for $D_R \sim 0.1(2\pi\Delta\nu_Q)$ (aligned sample, Figure 3C) and $D_R = 0.23(2\pi\Delta\nu_Q)$ (isotropic sample, Figure 3D, where $D_R = R/2$ (Samulski & Luz, 1980)). The translational diffusion constant for D_2O in our sample is not known, but any approximation can be obtained from the measurement by Lahajhar et al. (1981). They determined the diffusion coefficient at T = 25 °C for DNA hydrated at 86.5% relative humidity [~26 H_2O molecules/base pair (Brandes et al., 1986)] to be $D_T = 4.2 \times 10^{-6}$ cm^2 s^{-1}. Correcting for the temperature difference (but not for viscosity changes) gives $D_T = 3.7 \times 10^{-6}$ cm^2 s^{-1} at T = −11 °C. The calculated pitch length (diffusion along pitch axis only) is then P = 2.7 μm, in close accordance with the optical measurements. For the case of the isotropically ordered domains we find an average diffusion length of 1.8 μm. The diameter of the cholesteric units in the unaligned sample are therefore of the same order as the pitch length.

Conclusions. The studies discussed above demonstrate that short DNA fragments form a cholesteric liquid crystal at sufficiently high concentrations. The formation of this phase depends on factors such as temperture, salt concentration, DNA concentration, and length of DNA fragments. The observation that the DNA liquid crystals can be oriented in the magnetic field of an NMR magnet has not been previously reported, although there has been an earlier NMR study of concentrated DNA solutions comparable to those studied here (Rill et al., 1983). The fact that DNA molecules can be oriented by application of a magnetic field should prove to be useful in various spectroscopic studies of DNA structure and dynamics. In preliminary experiments we have been able to observe resonances from DNA deuterated in the 8-position of G and A in the liquid crystalline state. Earlier attempts to observe these resonances from DNA in more dilute solutions have been unsuccessful due to unfavorable relaxation conditions (Bendel et al., 1983; Brandes et al., 1986).

After our work was completed, Rill (1986) reported an extensive microscopic study of the textures of DNA liquid crystals in which he also worked out the phase diagram for the isotropic and liquid crystal phases of DNA in 2 M NaCl. Under comparable experimental conditions, our textures appear to be similar to those he reported. Moreover, our experiments clearly indicate that the liquid crystal phase is cholesteric.

ACKNOWLEDGMENTS

We thank Dr. Jack Opdycke and Tom Novet for help in preparing the samples. We are very grateful to Drs. Robert L. Vold and Regitze R. Vold for the use of their ^{2}H NMR spectrometer (construction supported by NSF Grant CHE 82-22097) and for the many helpful discussions.

REFERENCES

Bendel, P., Murphy-Boesh, J., & James, T. L. (1983) *Biochim. Biophys. Acta 759*, 205–213.

Brandes, R., Vold, R. R., Vold, R. L., & Kearns, D. R. (1986) *Biochemistry* (submitted for publication).

Chidichimo, G., Yaniv, Z., Vaz, N. A. P., & Doane, J. W. (1982) *Phys. Rev. A 25*, 1077–1083.

Collings, P. J., & McColl, J. R. (1978) *J. Chem. Phys. 69*, 3371–3373.

Davis, J. H., Jeffrey, K. R., Bloom, M., & Valic, M. I. (1976) *Chem. Phys. Lett. 42*, 390–394.

Demas, D., & Richter, L. (1978) in *Texture of Liquid Crystals*, plate 21, Verlag Chemie, Weinheim and New York.

DuPre, D. B., & Samulski, E. T. (1979) in *Liquid Crystals—The Forth State of Matter* (Saeva, F. D., Ed.) pp 203–297, Dekker, New York.

Falk, M., Poole, A. G., & Goymour, C. G. (1970) *Can. J. Chem. 48*, 1536–542.

Fowles, G. R. (1975) in *Introduction to Modern Optics*, 2nd ed., p 123, Holt, Rinehart and Winston, New York.

Fried, M. G., & Bloomfield, V. A. (1984) *Biopolymers 23*, 2141–2155.

Granot, J., Assa-Munt, N., & Kearns, D. R. (1982) *Biopolymers 21*, 873–883.

Halle, B., & Wennerström, H. (1981) *J. Chem. Phys. 75*, 1928–1943.

Helfrich, W. (1979) *J. Phys. Colloq. 40*, C3–105.

Iizuka, E. (1977) *Polym. J. 9*, 173–180.

Iizuka, E. (1978a) *Polym. J. 10*, 235–237.

Iizuka, E. (1978b) *Polym. J. 10*, 293–300.

Iizuka, E., & Yang, J. T. (1978) *Liq. Cryst. Ordered Fluids 3*, 197–207.

Iizuka, E., & Kondo, Y. (1979) *Mol. Cryst. Liq. Cryst. 51*, 285–294.

Lahajhar, G., Zupancic, I., & Rupprecht, A. (1982) in *Biophysics of Water* (Franks, F., Ed.) Wiley, New York.

Luz, Z., Poupko, R., & Samulski, E. T. (1981) *J. Chem. Phys. 74*, 5825–5837.

Onsager, L. (1949) *Ann. N.Y. Acad. Sci. 51*, 627–659.

Rill, R. L. (1986) *Proc. Natl. Acad. Sci. U.S.A. 83*, 342–346.

Biochemistry **1986**, *25*, 5895–5902 5895

Rill, R. L., Hilliard, P. R., & Levy, G. C. (1983) *J. Biol. Chem. 258*, 250–256.

Robinson, C. (1961) *Tetrahedron 13*, 219–234.

Rupprecht, A., & Forslind, B. (1970) *Biochim. Biophys. Acta 204*, 304–316.

Samulski, E. T., & Luz, Z. (1980) *J. Chem. Phys. 73*, 142–147.

Senechal, E., Maret, G., & Dransfeld, K. (1980) *Int. J. Biol. Macromol. 2*, 256–262.

Tanford, C. (1961) in *Physical Chemistry of Macromolecules*, Wiley, New York.

Trohalaki, S., Brian, A. A., Frisch, H. L., & Lerman, L. S. (1984) *Biophys. J. 45*, 777–782.

Vold, R. R., Brandes, R., Tsang, P., Kearns, D. R., Vold, R. L., & Rupprecht, A. (1986) *J. Am. Chem. Soc. 108*, 302–303.

Waldenstein, P., Rabidean, S. W., & Jackson, J. A. (1964) *J. Chem. Phys. 41*, 3407–3411.

Thermostability of Double-Stranded Deoxyribonucleic Acids: Effects of Covalent Additions of a Psoralen[†]

Yun-bo Shi and John E. Hearst[*]

Department of Chemistry, University of California, Berkeley, Berkeley, California 94720

Received April 25, 1986; Revised Manuscript Received June 24, 1986

ABSTRACT: We have carried out a thermodynamic study on the effects of covalent additions of the psoralen derivative HMT, 4′-(hydroxymethyl)-4,5′,8-trimethylpsoralen, on the stability of double-stranded deoxyoligonucleotides. This was done with two systems. The first was a double-stranded DNA formed by two non-self-complementary oligonucleotides, 5′-GAAGCTACGAGC-3′ and 5′-GCTCGTAGCTTC-3′, where we site specifically placed an HMT molecule on the thymidine residue in oligonucleotide 5′-GAAGCTACGAGC-3′ as either a furan-side monoadduct or a pyrone-side monoadduct. The second was a double-stranded DNA formed by a self-complementary oligonucleotide, 5′-GGGTACCC-3′, where we placed an HMT molecule on the thymidine residue of each strand as a furan-side monoadduct or cross-linked the two strands with an HMT molecule linked to the two thymidines. We found that HMT cross-linking of the two strands stabilizes the double helix formed by 5′-GGGTACCC-3′, as one might expect. Less predictable results were that the monoaddition of a psoralen stabilizes the double helix formed by the two non-self-complementary oligonucleotides by as much as 1.3 kcal/mol as a furan-side monoadduct and 0.7 kcal/mol as a pyrone-side monoadduct at 25 °C in 50 mM NaCl. In contrast, the monoaddition of a psoralen on each of the two thymidines in the double helix formed by 5′-GGGTACCC-3′ destabilizes the helix by 1.8 kcal/mol at 25 °C in 1 M NaCl. This destabilization arises from an unfavorable enthalpy change (8.6 kcal/mol) and a favorable entropy change (23 cal/K·mol) due to the two HMT molecules at the centers of each strand. The measured hypochromicity on helix formation also suggests a substantial perturbation in stacking interactions when one HMT is added to each of the two thymidines in the double helix.

Because of their photoreactivity with pyrimidine bases in double-stranded nucleic acids, psoralens (furocoumarins) have been widely used as biochemical probes of nucleic acid structure [for reviews, see Song and Tapley (1979) and Cimino et al. (1985)] and as drugs in the treatment of skin diseases (Fitzpatrick et al., 1982; Parrish et al., 1982). The chemistry of psoralen–nucleic acid intractions is well understood (Song & Tapley, 1979; Cimino et al., 1985; Parsons, 1980). The initial step is the intercalation of psoralen molecules between base pairs in a double-stranded nucleic acid helix. Upon UV irradiation (320–400 nm) the intercalated psoralens can react with pyrimidine bases through cyclobutane addition to produce psoralen–pyrimidine monoadducts. Due to the bifunctional nature of psoralens, two kinds of monoadducts are formed: the furan-side monoadduct, M_{Fu},[1] which is formed through the cycloaddition between the 4′,5′ double bond of a psoralen and the 5,6 double bond of a pyrimidine base, and the pyrone-side monoadduct, M_{Py}, which is formed through the cycloaddition between the 3,4 double bond of a psoralen and the 5,6 double bond of a pyrimidine base. By absorbing a second photon, the furan-side monoadduct can be converted to a diadduct when it is located at a cross-linkable site, i.e., when there is an adjacent pyrimidine base located on the other strand for the photoreaction. The pyrone-side monoadduct does not absorb photons above 320 nm, so it cannot be converted to a diadduct at wavelengths between 320 and 400 nm. The structures of the adducts formed between thymidine and several psoralen derivatives have been determined by techniques such as mass spectroscopy, proton NMR, and X-ray crystallography (Straub et al., 1982; Kanne et al., 1982a,b; Peckler et al., 1982).

[†] This work was supported by NIH Grant GM 11180.

[*] Author to whom correspondence should be addressed.

[1] Abbreviations: HMT, 4′-(hydroxymethyl)-4,5′,8-trimethylpsoralen; EtOH, ethanol; ATP, adenosine 5′-triphosphate; Tris, tris(hydroxymethyl)aminomethane; EDTA, ethylenediaminetetraacetic acid; M_{Fu}, furan-side monoadduct; M_{Py}, pyrone-side monoadduct; 5′-[T(HMT)$_{Fu}$]-3′, thymidine–HMT furan-side monoadduct with HMT on 3′-side of thymidine; 5′-[T(HMT)$_{Py}$]-3′, thymidine–HMT pyrone-side monoadduct with HMT on 3′-side of thymidine; T-HMT-T, thymidine–HMT–thymidine diadduct; T-HMT-C, thymidine–HMT–cytidine diadduct; C-HMT-C, cytidine–HMT–cytidine diadduct.

0006-2960/86/0425-5895$01.50/0